Chinese Journal of Physiology 60(3): 174-182, 2017
DOI: 10.4077/CJP.2017.BAF482

Effect of Methoxsalen on Ca^{2+} Homeostasis and Viability in Human Osteosarcoma Cells

Yi-Chau Lu[1, #], Chiang-Ting Chou[2, 3, #], Wei-Zhe Liang[4, #], Chun-Chi Kuo[5], Shu-Shong Hsu[6], Jue-Long Wang[7], and Chung-Ren Jan[4]

[1] Department of Orthopedics, Kaohsiung Veterans General Hospital, Kaohsiung 81362, Taiwan
[2] Department of Nursing, Division of Basic Medical Sciences, Chang Gung University of Science and Technology, Chia-Yi 61363, Taiwan
[3] Chronic Diseases and Health Promotion Research Center, Chang Gung University of Science and Technology, Chia-Yi 61363, Taiwan
[4] Department of Medical Education and Research, Kaohsiung Veterans General Hospital, Kaohsiung 81362, Taiwan
[5] Department of Nursing, Tzu Hui Institute of Technology, Pingtung 92641, Taiwan
[6] Department of Surgery, Kaohsiung Veterans General Hospital, Kaohsiung 81362, Taiwan
and
[7] Department of Rehabilitation, Kaohsiung Veterans General Hospital Tainan Branch, Tainan 71051, Taiwan, Republic of China

Abstract

Methoxsalen is a natural compound found in many seed plants. The effect of methoxsalen on Ca^{2+}-related physiology in human osteosarcoma is unclear. This study investigated the effect of methoxsalen on cytosolic free Ca^{2+} concentrations ($[Ca^{2+}]_i$) in MG63 human osteosarcoma cells. Methoxsalen induced $[Ca^{2+}]_i$ rises concentration-dependently. Methoxsalen-induced Ca^{2+} entry was confirmed by Mn^{2+}-induced quench of fura-2 fluorescence. This Ca^{2+} entry was suppressed by nifedipine, econazole, and SKF96365. In Ca^{2+}-free medium, incubation with the endoplasmic reticulum Ca^{2+} pump inhibitor 2,5-di-tert-butylhydroquinone (BHQ) inhibited methoxsalen-evoked $[Ca^{2+}]_i$ rises by 96%. In contrast, incubation with methoxsalen abolished BHQ-evoked $[Ca^{2+}]_i$ rises. Inhibition of phospholipase C (PLC) with U73122 abolished methoxsalen-induced $[Ca^{2+}]_i$ rises. Methoxsalen was cytotoxic at 300-700 μM in a concentration-dependent fashion. Chelating cytosolic Ca^{2+} with 1,2-bis(2-aminophenoxy)ethane-N,N,N',N'-tetraacetic acid/acetoxymethyl ester (BAPTA/AM) did not prevent methoxsalen-induced cytotoxicity. Collectively, our data suggest that in MG63 cells, methoxsalen induced $[Ca^{2+}]_i$ rises by evoking PLC-dependent Ca^{2+} release from the endoplasmic reticulum, and Ca^{2+} entry *via* store-operated Ca^{2+} entry. Methoxsalen also induced Ca^{2+}-disassociated cell death.

Key Words: Ca^{2+}, endoplasmic reticulum, human osteosarcoma cells, methoxsalen, phospholipase C

Introduction

Methoxsalen (also called 8-methoxypsoralen or xanthotoxin) is a natural photoactive compound found in diverse seed plants. Chemically, methoxsalen belongs to a class of organic natural molecules known as furanocoumarins (10, 33). Many epidermal proliferative diseases can be treated by methoxsalen plus long wave ultraviolet A (UVA) (33). Methoxsalen is used to treat psoriasis, eczema, vitiligo, and

Corresponding authors: [1] Dr. Shu-Shong Hsu, Department of Surgery, Kaohsiung Veterans General Hospital, Kaohsiung 81362, Taiwan, R.O.C.; [2] Dr. Jue-Long Wang, Department of Rehabilitation, Kaohsiung Veterans General Hospital Tainan Branch, Tainan 71051, Taiwan, R.O.C. and [3] Dr. Chung-Ren Jan, Department of Medical Education and Research, Kaohsiung Veterans General Hospital, Kaohsiung 81362, Taiwan, R.O.C. Tel: +886-7-3422121 ext. 1509, Fax: +886-7-3468056, E-mail: crjan@isca.vghks.gov.tw
Received: November 3, 2016; Revised: January 13, 2017; Accepted: January 18, 2017.
 ISSN : 0304-4920. http://www.cps.org.tw

some cutaneous lymphomas in conjunction with exposing the skin to UVA light (33). Methoxsalen has been shown to exert different physiological effects on some models. *In vivo,* previous studies have shown that methoxsalen altered oogenesis (12) and acted as a cytochrome P450 2A5/6 inhibitor (1) in mice, inhibited cytochrome P450 2A13 in the human lung (43), and stimulated chloride secretion in the mouse jejunum (17). In cultured cells, methoxsalen induced cytotoxicity through apoptosis in HepG2 human hepatoma cells (30), human lymphocytes (37, 44), and NCTC-2544/HaCaT human keratinocytes (21, 42). Furthermore, methoxsalen caused cell cycle arrest in Karpas 299 human T-lymphoma cells (3), inhibited angiogenesis in dermal-derived normal human microvascular endothelial cells (HMVEC-d) (9), and upregulated levels of caspase-9 in Jurkat T leukemia cells (27). However, the effect of methoxsalen on Ca^{2+} homeostasis has not been explored in human osteosarcoma.

An elevation in cytosolic free Ca^{2+} concentrations ($[Ca^{2+}]_i$) is a pivotal messenger for numerous cellular processes including gene expression, fertilization, channel regulation, secretion, contraction, plasticity, proliferation and apoptosis (2, 36). Cells have many mechanisms to tightly regulate $[Ca^{2+}]_i$ (15, 26). A $[Ca^{2+}]_i$ rise can be due to Ca^{2+} influx from external solution or Ca^{2+} release from stores (19, 31). In osteosarcoma cells, the main Ca^{2+} influx pathway is the store-operated Ca^{2+} entry, which is triggered by depletion of the endoplasmic reticulum Ca^{2+} stores (19, 31). Activation of phospholipase C (PLC) leads to formation of inositol trisphosphate (IP_3). IP_3 subsequently activates the IP_3 receptors on the endoplasmic reticulum to release the stored Ca^{2+} (13). Many intracellular molecules can modulate a Ca^{2+} signal such as protein kinase C (PKC) (11), cyclic guanosine monophosphate (cGMP) (34) etc. To examine the action of methoxsalen on $[Ca^{2+}]_i$ in human osteosarcoma cells, the MG63 cell was used since it produces measurable $[Ca^{2+}]_i$ rises when stimulated by different chemicals including NPC-14686 (6), sertraline (24), and 3,3'-diindolylmethane (25).

To this end, fura-2 was applied as a Ca^{2+}-sensitive probe to assess $[Ca^{2+}]_i$. We have characterized the $[Ca^{2+}]_i$ rises, established the concentration-response relationship, and examined the pathways underlying methoxsalen-induced Ca^{2+} entry and Ca^{2+} release. Furthermore, the cytotoxic effect of methoxsalen and its relationship to Ca^{2+} were also investigated.

Materials and Methods

Chemicals

The chemicals for cell culture were purchased from Gibco® (Gaithersburg, MD, USA). Aminopolycarboxylic acid/acetoxy methyl (fura-2/AM) and 1,2-bis(2-aminophenoxy)ethane-N,N,N',N'-tetraacetic acid/acetoxymethyl ester (BAPTA/AM) were purchased from Molecular Probes® (Eugene, OR, USA). The other chemicals were purchased from Sigma-Aldrich® (St. Louis, MO, USA).

Cell Culture

MG63 human osteosarcoma cells purchased from Bioresource Collection and Research Center (Taiwan) were cultured in minimum essential medium (MEM) supplemented with 10% heat-inactivated fetal bovine serum, 100 U/ml penicillin and 100 μg/ml streptomycin.

Solutions for $[Ca^{2+}]_i$ Measurements

Ca^{2+}-containing medium (pH 7.4) had 140 mM NaCl, 5 mM KCl, 1 mM $MgCl_2$, 2 mM $CaCl_2$, 10 mM 4-(2-hydroxyethyl)-1-piperazineethanesulfonic acid (HEPES), and 5 mM glucose. Ca^{2+}-free medium had similar chemicals as Ca^{2+}-containing medium except that $CaCl_2$ was substituted with 0.3 mM ethylene glycol tetraacetic acid (EGTA) and 2 mM $MgCl_2$. Methoxsalen was dissolved in ethanol as a 2 M stock solution. The other chemicals were dissolved in water, ethanol or dimethyl sulfoxide (DMSO). The concentration of organic solvents in the experimental solutions was below 0.1%, and did not affect basal $[Ca^{2+}]_i$ or viability.

$[Ca^{2+}]_i$ Measurements

The $[Ca^{2+}]_i$ was measured as previously described (6, 24, 25). Confluent cells grown on 6 cm dishes were trypsinized and made into a suspension in culture medium at a concentration of 10^6/ml. Cell viability was determined by trypan blue exclusion (adding 0.2% trypan blue to 0.1 ml cell suspension). The viability was greater than 95% after the treatment. Cells were subsequently loaded with 2 μM fura-2/AM for 30 min at 25°C in the same medium. After loading, cells were washed with Ca^{2+}-containing medium twice and was made into a suspension in Ca^{2+}-containing medium at a concentration of 10^7/ml. Fura-2 fluorescence measurements were performed in a water-jacketed cuvette (25°C) with continuous stirring; the cuvette contained 0.5 million cells suspended in 1 ml of medium. Fluorescence was monitored with a Shimadzu RF-5301PC spectrofluorophotometer immediately after 0.1 ml cell suspension was added to 0.9 ml Ca^{2+}-containing or Ca^{2+}-free medium, by recording excitation signals at 340 nm and 380 nm and emission signal at 510 nm at 1 s intervals.

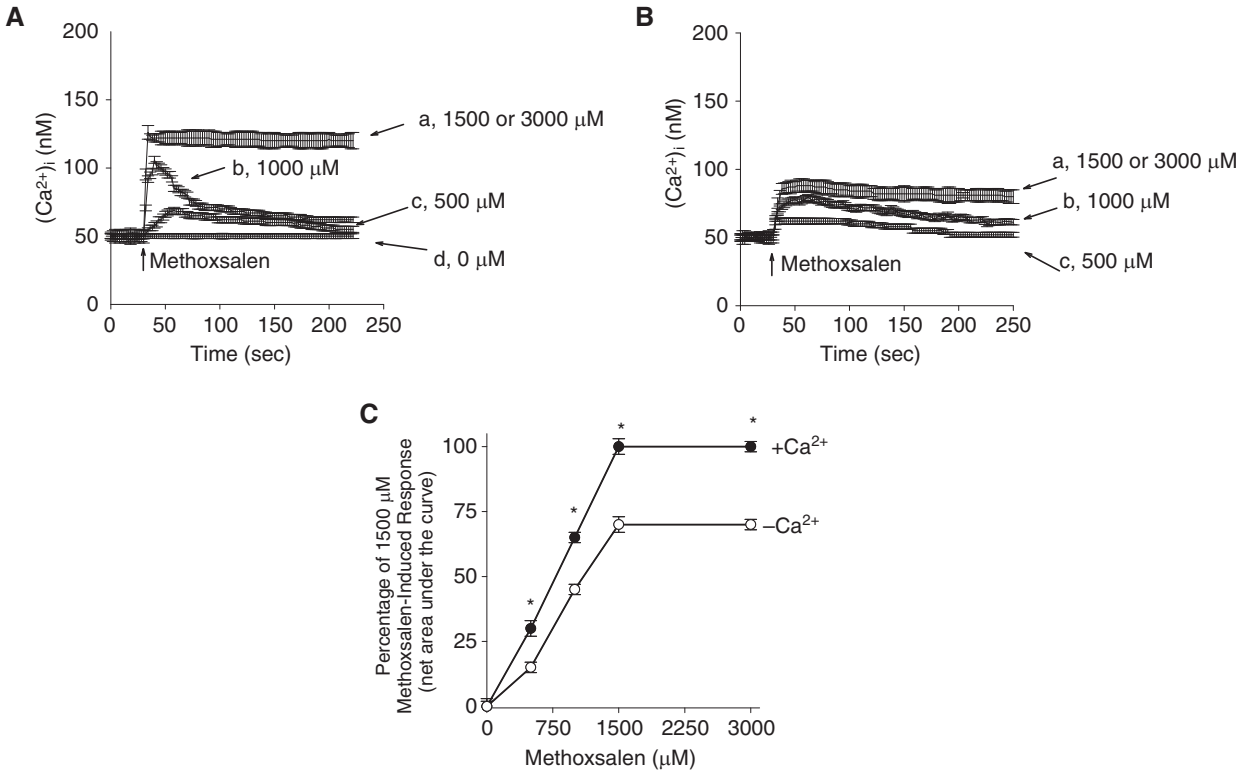

Fig. 1. Effect of methoxsalen on $[Ca^{2+}]_i$ in fura-2-loaded MG63 cells. (A) Methoxsalen was added at 25 s. The concentration of methoxsalen was indicated. The experiments were performed in Ca^{2+}-containing medium. (B) Effect of methoxsalen on $[Ca^{2+}]_i$ in the absence of extracellular Ca^{2+}. Methoxsalen was added at 25 s in Ca^{2+}-free medium. (C) Concentration-response plots of methoxsalen-induced $[Ca^{2+}]_i$ rises in the presence or absence of extracellular Ca^{2+}. Y axis is the percentage of the net (baseline subtracted) area under the curve (25-250 s) of the $[Ca^{2+}]_i$ rises induced by 1500 μM methoxsalen in Ca^{2+}-containing medium. Data are mean ± standard error of the mean (SEM) of three experiments. *$P < 0.05$: compared to open circles.

For calibration of $[Ca^{2+}]_i$, after completion of the experiments, Triton X-100 (0.1%) and $CaCl_2$ (5 mM) were added to the cuvette to obtain the maximal fura-2 fluorescence (6, 16, 24, 25). The Ca^{2+} chelator EGTA (10 mM) was subsequently added to chelate Ca^{2+} in the cuvette to obtain the minimal fura-2 fluorescence. Control experiments showed that cells bathed in a cuvette had a viability of 95% after 20 min of fluorescence measurements. $[Ca^{2+}]_i$ was calculated as previously described (16).

To assess Ca^{2+} entry, Mn^{2+} quenching of fura-2 fluorescence was performed in Ca^{2+}-containing medium containing 50 μM $MnCl_2$. $MnCl_2$ was added to cell suspension in the cuvette 30 sec before fluorescence recoding began. Data were recorded at excitation signal at 360 nm (Ca^{2+}-insensitive) and emission signal at 510 nm at 1-sec intervals as described previously (28).

Cell Viability Assays

Viability was explored as previously described (6, 24, 25). The assessment of cell viability was based on the rational that cells can cleave tetrazolium salts by dehydrogenases. Increases in the intensity of color correlated with the live cell number. Assays were conducted according to manufacturer's instructions (Roche Molecular Biochemical, Indianapolis, IN, USA). Cells were seeded in 96-well plates at a concentration of 10,000 cells/well in culture medium for 24 h in the presence of methoxsalen. The cell viability detecting tetrazolium reagent 4-[3-[4-Iodophenyl]-2-4(4-nitrophenyl)-2H-5-tetrazolio-1,3-benzene disulfonate] (WST-1; 10 μl pure solution) was added to samples after methoxsalen incubation, and cells were incubated for 30 min in a humidified atmosphere. In experiments using BAPTA/AM to chelate cytosolic Ca^{2+}, cells were incubated with 5 μM BAPTA/AM for 1 h before incubation with methoxsalen. The cells were washed once with Ca^{2+}-containing medium and incubated with/without methoxsalen for 24 h. The absorbance of samples (A_{450}) was determined using an enzyme-linked immunosorbent assay (ELISA) reader. Absolute optical density was normalized to the absorbance of untreated cells in each plate and expressed as a percentage of the control.

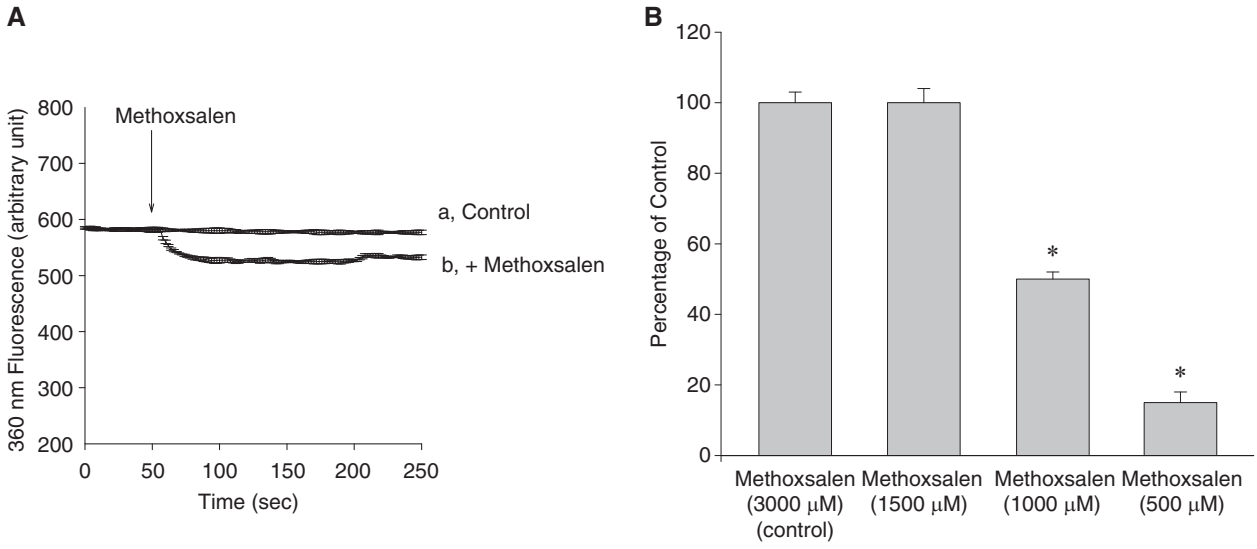

Fig. 2. Effect of methoxsalen on Ca^{2+} influx by measuring Mn^{2+} quenching of fura-2 fluorescence. Experiments were performed in Ca^{2+}-containing medium. (A) $MnCl_2$ (50 μM) was added to cells 1 min before fluorescence measurements. The y axis is fluorescence intensity (in arbitrary units) measured at the Ca^{2+}-insensitive excitation wavelength of 360 nm and the emission wavelength of 510 nm. Trace a: control, without methoxsalen. Trace b: methoxsalen (1500 μM) was added as indicated. (B) A bar graph showing the concentration-dependent effect of methoxsalen on Mn^{2+} quenching. Data are mean ± SEM of three separate experiments. *$P < 0.05$ compared to first bar.

Statistics

Data are shown as mean SEM of three independent experiments. Data were analyzed by one-way analysis of variances (ANOVA) using the Statistical Analysis System (SAS®, SAS Institute Inc., Cary, NC, USA). Multiple comparisons between group means were performed by *post-hoc* analysis using the Tukey's HSD (honestly significantly difference) procedure. A P value less than 0.05 was considered significant.

Results

Effect of Methoxsalen on $[Ca^{2+}]_i$

The basal $[Ca^{2+}]_i$ level was 51 ± 1 nM (Fig. 1A). Methoxsalen evoked $[Ca^{2+}]_i$ rises in a concentration-dependent manner at concentrations between 500 and 1500 μM in Ca^{2+}-containing medium. At a concentration of 1500 μM, methoxsalen evoked $[Ca^{2+}]_i$ rises that attained to a net increase of 71 ± 2 nM. In the absence of extracellular Ca^{2+}, 500-1500 μM methoxsalen evoked concentration-dependent $[Ca^{2+}]_i$ rises (Fig. 1B). The Ca^{2+} response saturated at 1500 μM methoxsalen because 3000 μM methoxsalen did not cause greater responses (Fig. 1A and 1B). The concentration-response relationship of methoxsalen-induced $[Ca^{2+}]_i$ rises were shown in Fig. 1C. The EC_{50} value was 652 ± 3 μM or 701 ± 2 μM in Ca^{2+}-containing medium or Ca^{2+}-free medium, respectively, by fitting to a Hill equation.

Methoxsalen-Induced Mn^{2+} Influx

Mn^{2+} and Ca^{2+} share similar pathways of entering cells but the former quenches fura-2 fluorescence at all excitation wavelengths (28). Thus, Ca^{2+} entry can be indirectly demonstrated by quenching of fura-2 fluorescence excited at the Ca^{2+}-insensitive excitation wavelength of 360 nm by Mn^{2+}. Since methoxsalen-induced Ca^{2+} response saturated at 1500 μM, in the following experiments the response induced by 1500 μM methoxsalen was used as control. Figure 2 shows that 1500 μM methoxsalen evoked an instant decrease in the 360 nm excitation signal that reached a maximum value of 61 ± 1 arbitrary units at 100 s. Furthermore, methoxsalen induced Mn^{2+} quenching in a concentration-dependent manner (Fig. 2B). The Mn^{2+} quenching results imply that Ca^{2+} entry contributed to methoxsalen-induced Ca^{2+} signal. Moreover, it suggests that store-operated Ca^{2+} entry occurred in methoxsalen-induced $[Ca^{2+}]_i$ rises.

Modulation of Methoxsalen-Induced $[Ca^{2+}]_i$ Rises

In Ca^{2+}-containing medium, three store-operated Ca^{2+} entry inhibitors: nifedipine (1 μM), econazole (0.5 μM) and SKF96365 (5 μM); phorbol 12-myristate 13 acetate (PMA; 1 nM; a protein kinase C, PKC activator); and GF109203X (2 μM; a PKC inhibitor) were added 1 min before methoxsalen (1500 μM). Except PMA and GF109203X, the other chemicals inhibited methoxsalen-induced $[Ca^{2+}]_i$ rises by

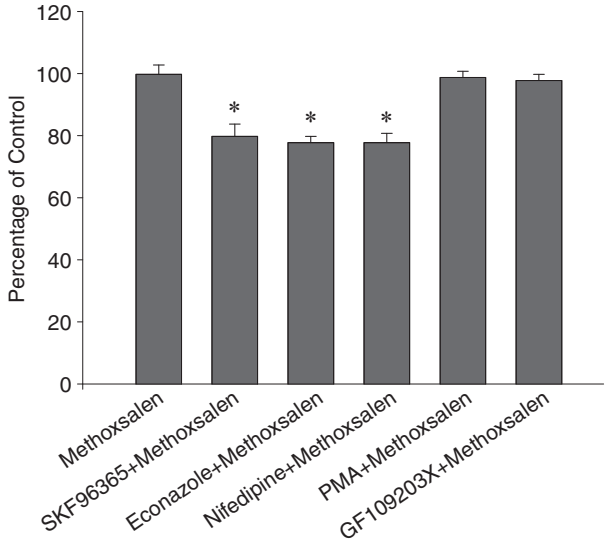

Fig. 3. Effect of Ca^{2+} channel modulators on methoxsalen-induced $[Ca^{2+}]_i$ rises. In blocker- or modulator-treated groups, the reagent was added 1 min before methoxsalen (1500 μM). The concentration was 1 μM for nifedipine, 0.5 μM for econazole, 5 μM for SKF96365, 10 nM for PMA, and 2 μM for GF109203X. Data are expressed as the percentage of control (1st column, 100%) that is the area under the curve (25-200 s) of 1500 μM methoxsalen-induced $[Ca^{2+}]_i$ rises in Ca^{2+}-containing medium, and are mean ± SEM of three separate experiments. *P < 0.05 compared to the 1st column. Data are mean ± SEM of three separate experiments.

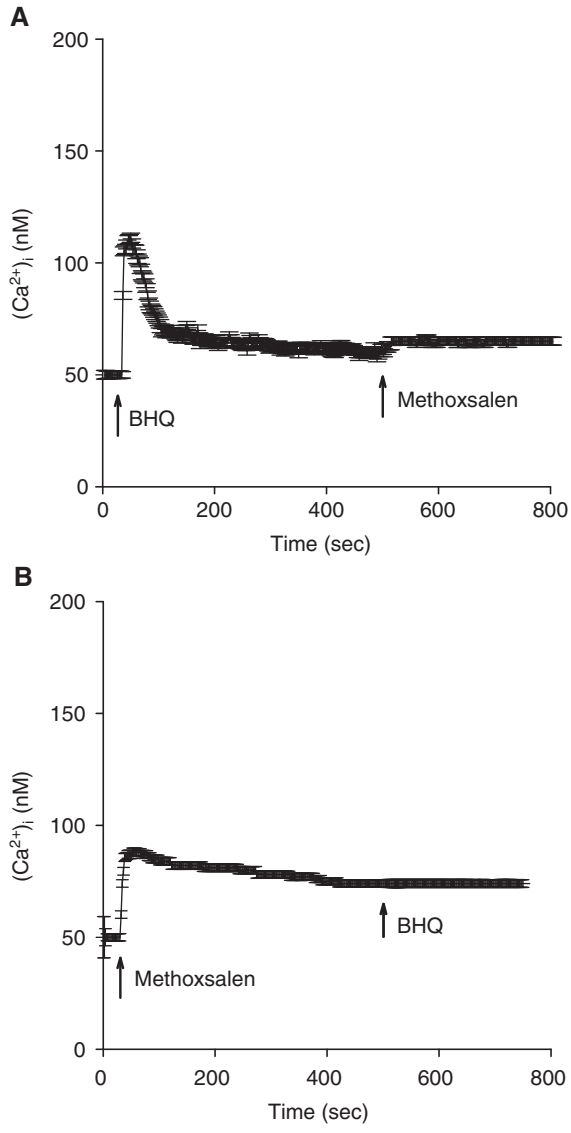

Fig. 4. Effect of BHQ on methoxsalen-induced Ca^{2+} release. (A)(B) BHQ (50 μM) and methoxsalen (1500 μM) were added at time points indicated. Experiments were performed in Ca^{2+}-free medium. Data are mean ± SEM of three separate experiments.

approximately 20% (Fig. 3). This suggests that store-operated Ca^{2+} entry involved in methoxsalen-induced $[Ca^{2+}]_i$ rises.

The Source of Methoxsalen-Induced Ca^{2+} Release

The endoplasmic reticulum has been shown to be a dominant Ca^{2+} store in most cell types (4, 8). Therefore the role of the endoplasmic reticulum in methoxsalen-induced Ca^{2+} release in MG63 cells was explored. To exclude the contribution of Ca^{2+} entry, the experiments were performed in Ca^{2+}-free medium. Fig. 4A shows that addition of 50 μM 2,5-di-tert-butylhydroquinone (BHQ), an endoplasmic reticulum Ca^{2+} pump inhibitor (41), evoked $[Ca^{2+}]_i$ rises of 59 ± 2 nM. Subsequently added 1500 μM methoxsalen induced small $[Ca^{2+}]_i$ rises of 3 ± 2 nM. Fig. 4B shows that addition of BHQ failed to release more Ca^{2+} after methoxsalen-induced $[Ca^{2+}]_i$ rises.

A Role of PLC in Methoxsalen-Induced $[Ca^{2+}]_i$ Rises

The protein PLC plays a crucial role in regulating the release of Ca^{2+} from the endoplasmic reticulum (4, 8). Since our data show that methoxsalen released Ca^{2+} from the endoplasmic reticulum, the involvement of PLC in this process was examined. U73122 (38) is a commonly used PLC inhibitor, thus was applied to examine if the activation of this enzyme was needed for methoxsalen-induced Ca^{2+} release. Firstly, Fig. 5A shows that adenosine triphosphate (ATP) (10 μM) was found to evoke $[Ca^{2+}]_i$ rises of 25 ± 2 nM. Because ATP is a PLC-dependent agonist of $[Ca^{2+}]_i$ rises in most cell types (14), U73122 was used to test its inhibitory effect on ATP-induced $[Ca^{2+}]_i$ rises. Figs. 5A and 5B show that incubation with U73122 (2 μM) did not alter basal $[Ca^{2+}]_i$ but completely inhibited ATP-induced $[Ca^{2+}]_i$ rises. This suggests that U73122 effectively suppressed PLC activity. Subsequently, the

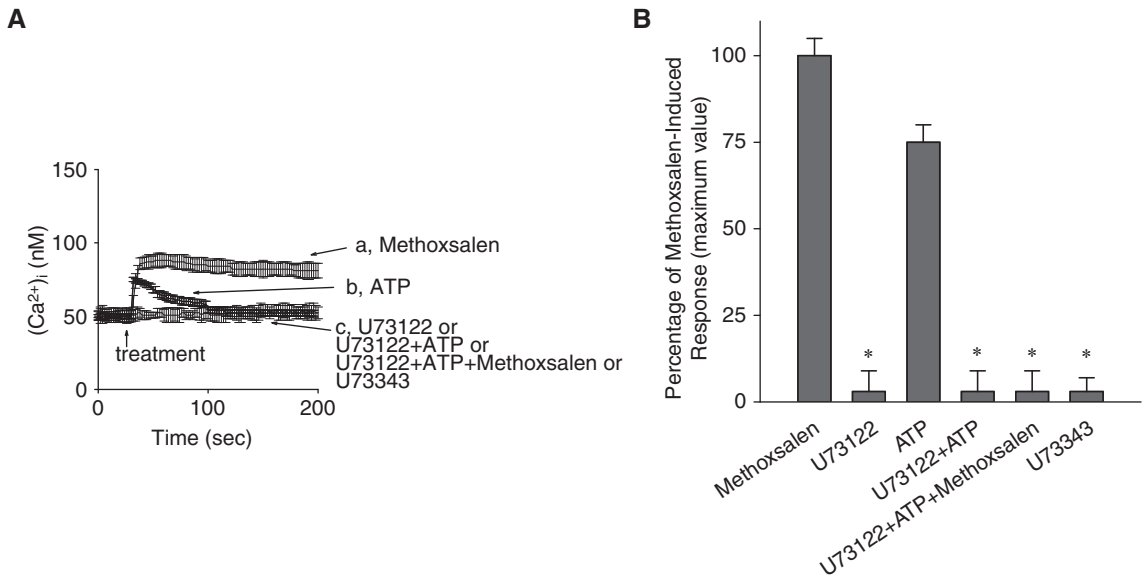

Fig. 5. Effect of U73122 on methoxsalen-induced Ca^{2+} release. Experiments were performed in Ca^{2+}-free medium. (A) Trace a: methoxsalen (1500 μM) was added at 30 sec. Trace b: ATP (10 μM) was added at 30 sec. Trace c: this trace contained four recordings which overlapped. These recordings were: 1, U73122 (2 μM) was added at 30 sec. 2, U73122 (2 μM) was added at 30 sec followed by ATP (10 μM) at 60 sec. 3, U73122 (2 μM) was added at 30 sec followed by ATP at 60 sec and methoxsalen (1500 μM) at 100 sec. 4, U73343 (2 μM) was added at 30 sec. (B) U73122 (2 μM), ATP, and methoxsalen (1500 μM) were added as indicated. Data are mean ± SEM of three separate experiments. *$P < 0.05$ compared to first bar (control). Control is the area under the curve of 1500 μM methoxsalen-induced $[Ca^{2+}]_i$ rises (25-190 s).

data show that incubation with 2 μM U73122 did not alter basal $[Ca^{2+}]_i$ but abolished 1500 μM methoxsalen-induced $[Ca^{2+}]_i$ rises. Although U73122 is generally deemed as a selective inhibitor of PLC, the possibility that U73122 acted by PLC-independent action needs to be excluded. Thus U73343 was used as a negative control. U73343 is structurally very similar to U73122 while lacks inhibitory effect on PLC. Our results show that U73343 (2 μM) failed to alter ATP-induced $[Ca^{2+}]_i$ rises (Fig. 5, A and B). Therefore, this most likely suggests that U73122 selectively in hibited PLC activity in methoxsalen-induced $[Ca^{2+}]_i$ rises. Furthermore, it supports that store-operated Ca^{2+} channels participated in methoxsalen-induced Ca^{2+} release.

Effect of Methoxsalen on Cell Viability

Methoxsalen (0-700 μM) was added to cells for 24 h, and tetrazolium assay was performed. Methoxsalen caused a decrease in viability in a concentration-dependent manner between 300-700 μM (Fig. 6). Because methoxsalen significantly induced $[Ca^{2+}]_i$ rises, the next question was whether methoxsalen-caused cytotoxicity was induced by preceding $[Ca^{2+}]_i$ rises. The intracellular Ca^{2+} chelator BAPTA/AM (5 μM) (40) was applied to prevent $[Ca^{2+}]_i$ rises during methoxsalen incubation. At a concentration of 1500 μM, methoxsalen did not evoke $[Ca^{2+}]_i$ rises in BAPTA-AM-treated cells (not shown). Fig. 6 shows that 5 μM BAPTA-AM incubation did not change viability of control cell. In the presence of 300-700 μM methoxsalen, BAPTA-AM loading did not reverse methoxsalen-induced cell death. Thus, the findings implicate that methoxsalen-evoked cytotoxicity was not caused by $[Ca^{2+}]_i$ rises.

Discussion

Ca^{2+} signaling plays a key role in numerous cellular responses. In this regard, literature shows that methoxsalen affected Ca^{2+} signaling and regulated physiology in GH4C1 rat pituitary cells (29) or rabbit corpus cavernosum (7). However, the pathways underlying this Ca^{2+} signaling was not completely elucidated. The present study shows that methoxsalen induced $[Ca^{2+}]_i$ rises in MG63 cells by releasing Ca^{2+} stores and inducing Ca^{2+} entry. Removal of extracellular Ca^{2+} partly inhibited methoxsalen-induced Ca^{2+} entry throughout the measurement of 200 s, suggesting that both methoxsalen induced both Ca^{2+} entry and Ca^{2+} release. The Mn^{2+} quenching results also implicate that Ca^{2+} entry contributed to methoxsalen-induced Ca^{2+} signal.

The pathway of methoxsalen-induced Ca^{2+} entry was examined. In many cells including MG63 cells, store-operated Ca^{2+} channels have been shown to play a crucial role in $[Ca^{2+}]_i$ rises triggered by different compounds such as NPC-14686 (6) and setraline (24). Despite that there are so far no selective inhibitors for this Ca^{2+} entry, nifedipine, econazole and SKF96365

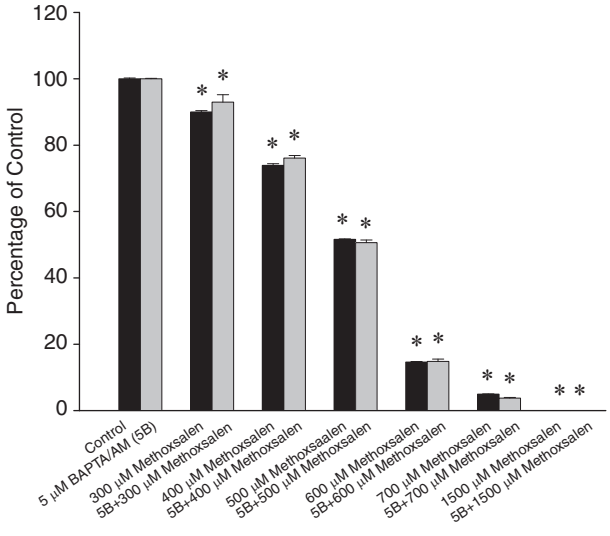

Fig. 6. Methoxsalen-induced Ca^{2+}-independent cell death. Cells were treated with 0-1500 μM methoxsalen for 24 h, and the cell viability assay was performed. Data are mean ± SEM of three separate experiments. Each treatment had six replicates (wells). Data are expressed as percentage of control that is the increase in cell numbers in methoxsalen-free groups. Control had 10,775 ± 712 cells/well before experiments, and had 13,566 ± 788 cells/well after incubation for 24 h. $*P < 0.05$ compared to control. In each group, the Ca^{2+} chelator BAPTA-AM (5 μM) was added to cells followed by treatment with methoxsalen in Ca^{2+}-containing medium. Data are expressed as the percentage of control (in methoxsalen-free groups, 100%). Cell viability assay was subsequently performed.

were commonly applied for this purpose (18, 20, 32, 35). Our results suggest that all of these three chemicals inhibited methoxsalen-induced $[Ca^{2+}]_i$ rises. Therefore methoxsalen-induced Ca^{2+} entry appears to involve store-operated Ca^{2+} pathway.

The changes of the activity of protein kinases are well established to be able to alter Ca^{2+} signaling (4, 5, 11). However, our findings suggest that methoxsalen-induced $[Ca^{2+}]_i$ rises were not changed by the status of PKC activity. This suggests that PKC may not be involved in methoxsalen-induced Ca^{2+} signaling. The next question was the identity of the Ca^{2+} stores responsible for methoxsalen-induced Ca^{2+} release. Our data suggest that the endoplasmic reticulum stores appeared to be dominant in this response. The endoplasmic reticulum is the major intracellular Ca^{2+} stores of cells, whereas mitochondria shape and decode cellular Ca^{2+} signals by taking up and then releasing Ca^{2+} ions (4, 8). A mitochondrial Ca^{2+} channel known as the uniporter drives the rapid and massive entry of Ca^{2+} ions into mitochondria. The uniporter operates at high, micromolar $[Ca^{2+}]_i$ that are only reached transiently in cells, near Ca^{2+} release channels (4, 8). The results show that incubation with the endoplasmic reticulum Ca^{2+} pump inhibitor BHQ inhibited 95% of methoxsalen-induced $[Ca^{2+}]_i$ rises. In contrast, incubation with methoxsalen abolished BHQ-induced $[Ca^{2+}]_i$ rises. The residual 5% might be contributed by other stores such as mitochondria, cytosketolon or nucleus, etc. (4, 8).

The data further show that the Ca^{2+} release was *via* a PLC-dependent mechanism, because it was abolished when PLC activity was inhibited. G protein–coupled receptors (GPCRs) constitute a large protein family of receptors that sense molecules outside the cell and activate inside signal transduction pathways and, ultimately, cellular responses (4, 8). The PLC signal pathway is a principal signal transduction of the GPCRs (4, 8). Because the data show that methoxsalen induced $[Ca^{2+}]_i$ rises by evoking PLC-dependent Ca^{2+} release from the endoplasmic reticulum. Therefore it suggests that methoxsalen may act on GPCRs.

Methoxsalen (300-700 μM) was found to be cytotoxic to MG63 cells in a concentration-dependent manner. It has been established that Ca^{2+} overload can trigger diverse processes resulting in changes in cell viability (4, 8). One possible explanation for methoxsalen-induced cytotoxicity in MG63 cells was that Ca^{2+} played a role in the cell death. However, our data show that 300-700 μM methoxsalen-induced cell death was not reversed when cytosolic Ca^{2+} was chelated by BAPTA-AM. This implies that in this case, methoxsalen-induced cell death was not triggered by $[Ca^{2+}]_i$ rises.

Viability and $[Ca^{2+}]_i$ assays were different in the method. In viability assays, cells were incubated with methoxsalen for 24 h in order to gain significant changes in viability. In contrast, $[Ca^{2+}]_i$ assays were performed online and terminated within 10 min, and trypan blue exclusion showed that after treatment with methoxsalen, cell viability was still >95%. This explains 700 μM methoxsalen decreased cell viability by approximately 95% while 1500 μM methoxsalen did not alter viability in $[Ca^{2+}]_i$ assays.

The pharmacokinetics and availability of methoxsalen *in vivo* were explored in several studies. The plasma level of methoxsalen may reach 20-50 μM (39, 45). This level may be expected to go much higher in patients with liver or kidney disorders or taking higher doses (39, 45). Furthermore, in previous studies, pretreatment with methoxsalen (250 μmol/kg) appears to decrease the metabolic activation of chloroform and essentially prevents its hepatotoxicity and nephrotoxicity in mice (22, 23). However, our data show that methoxsalen at a concentration of 300 μM induced slight cell death. Many anticancer drugs have poor and highly variable oral bioavailability. As pharmacokinetics plays a very important role in determining drug dose, exposure, and drug activity, an

improved pharmacokinetic profile would result in enhanced antitumor activity and decreased systemic toxicity. Thus, the development of orally administrable anticancer drugs is receiving increased attention to improve the physicochemical and pharmacokinetic profiles of newly designed molecules. Because chemical modifications or more formulations that can bypass their poor oral bioavailability have been developed, it is important to explore structure-activity relationship studies to improve efficacy and potency. Since methoxsalen and its metabolites have therapeutic potential against cancers, advanced drug delivery systems for enhanced bioavailability and mechanisms to maintain effective therapeutic concentrations in the blood should also be considered.

Ca^{2+} signaling is involved in many cellular processes, such as cell death, differentiation, proliferation, and survival. The Ca^{2+} signaling pathway and its biological significance have not yet been examined in methoxsalen-treated human oseteosarcoma cells. This study shows that in MG63 human osteosarcoma cells, the natural photoactive compound methoxsalen, caused Ca^{2+} influx *via* store-operated Ca^{2+} entry and induced Ca^{2+} release from the endoplasmic reticulum in a PLC-dependent manner. Methoxsalen induced cytotoxicity independently of preceding $[Ca^{2+}]_i$ rises. The $[Ca^{2+}]_i$-elevating and cytotoxic effects of methoxsalen should be taken into account in performing other *in vitro* studies.

Conflict of Interest

The authors declared no conflicts of interest.

Acknowledgements

This work was supported by VGHKS104-079 to Lu YC.

References

1. Alsharari, S.D., Siu, E.C., Tyndale, R.F. and Damaj, M.I. Pharmacokinetic and pharmacodynamics studies of nicotine after oral administration in mice: effects of methoxsalen, a CYP2A5/6 inhibitor. *Nicotine Tob. Res.* 16: 18-25, 2014.
2. Baba, Y., Matsumoto, M. and Kurosaki, T. Calcium signaling in B cells: Regulation of cytosolic Ca^{2+} increase and its sensor molecules, STIM1 and STIM2. *Mol. Immunol.* 62: 339-343, 2014.
3. Bartosová, J., Kuzelová, K., Pluskalová, M., Marinov, I., Halada, P. and Gasová, Z. UVA-activated 8-methoxypsoralen (PUVA) causes G2/M cell cycle arrest in Karpas 299 T-lymphoma cells. *J. Photochem. Photobiol. B* 85: 39-48, 2006.
4. Bootman, M.D., Berridge, M.J. and Roderick, H.L. Calcium signalling: more messengers, more channels, more complexity. *Curr. Biol.* 12: R563-R565, 2002.
5. Bynagari-Settipalli, Y.S., Lakhani, P., Jin, J., Bhavaraju, K., Rico, M.C., Kim, S., Woulfe, D. and Kunapuli, S.P. Protein kinase C isoform ε negatively regulates ADP-induced calcium mobilization and thromboxane generation in platelets. *Arterioscler. Thromb. Vasc. Biol.* 32: 1211-1219, 2010.
6. Chien, J.M., Chou, C.T., Liang, W.Z., Kuo, D.H., Kuo, C.C., Ho, C.M., Shieh, P. and Jan, C.R. The Mechanism of NPC-14686-induced $[Ca^{2+}]_i$ rises and non-Ca^{2+}-triggered cell Death in MG63 human osteosarcoma cells. *Chinese J. Physiol.* 57: 158-166, 2014.
7. Chiou, W.F., Huang, Y.L., Chen, C.F. and Chen, C.C. Vasorelaxing effect of coumarins from Cnidium monnieri on rabbit corpus cavernosum. *Planta Med.* 67: 282-284, 2001.
8. Clapham, D.E. Intracellular calcium. Replenishing the stores. *Nature* 375: 634-635, 1995.
9. Deng, H., Yan, C.L., Hu, Y., Xu, Y. and Liao, K.H. Photochemotherapy inhibits angiogenesis and induces apoptosis of endothelial cells *in vitro*. *Photodermatol. Photoimmunol. Photomed.* 20: 191-199, 2004.
10. de Wolff, F.A. and Thomas, T.V. Clinical pharmacokinetics of methoxsalen and other psoralens. *Clin. Pharmacokinet.* 11: 62-75, 1986.
11. Dougherty, P.J., Nepiyushchikh, Z.V., Chakraborty, S., Wang, W., Davis, M.J., Zawieja, D.C. and Muthuchamy, M. PKC activation increases Ca^{2+} sensitivity of permeabilized lymphatic muscle *via* myosin light chain 20 phosphorylation-dependent and -independent mechanisms. *Am. J. Physiol. Heart Circ. Physiol.* 306: H674-H683, 2014.
12. Farhadi, M., Fattahi, E., Mohseni Kouchesfahani, H., Shockravi, A. and Parivar, K. The adverse effects of methoxsalen on the oogenesis of Balb/C mice. *Cell J.* 15: 348-355, 2014.
13. Fedorenko, O.A., Popugaeva, E., Enomoto, M., Stathopulos, P.B., Ikura, M. and Bezprozvanny, I. Intracellular calcium channels: inositol-1,4,5-trisphosphate receptors. *Eur. J. Pharmacol.* 739: 39-48, 2014.
14. Florenzano, F., Viscomi, M.T., Mercaldo, V., Longone, P., Bernardi, G., Bagni, C., Molinari, M. and Carrive, P. P2X2R purinergic receptor subunit mRNA and protein are expressed by all hypothalamic hypocretin/orexin neurons. *J. Com. Neurol.* 498: 58-67, 2006.
15. Gómez, A.M., Ruiz-Hurtado, G., Benitah, J.P. and Domínguez-Rodríguez, A. Ca^{2+} fluxes involvement in gene expression during cardiac hypertrophy. *Curr. Vasc. Pharmacol.* 11: 497-506, 2013.
16. Grynkiewicz, G., Poenie, M. and Tsien, R.Y. A new generation of Ca^{2+} indicators with greatly improved fluorescence properties. *J. Biol. Chem.* 260: 3440-3450, 1985.
17. Hamilton, K.L., Butt, A.G., Cheng, S. and Carter, D.J. Methoxsalen stimulates electrogenic Cl^- secretion in the mouse jejunum. *Exp. Physiol.* 87: 437-445, 2002.
18. Ishikawa, J., Ohga, K., Yoshino, T., Takezawa, R., Ichikawa, A., Kubota, H. and Yamada, T. A pyrazole derivative, YM-58483, potently inhibits store-operated sustained Ca^{2+} influx and IL-2 production in T lymphocytes. *J. Immunol.* 170: 4441-4449, 2009.
19. Izquierdo, J.H., Bonilla-Abadía, F., Cañas, C.A. and Tobón, G.J. Calcium, channels, intracellular signaling and autoimmunity. *Reumatol. Clin.* 10: 43-47, 2014.
20. Jiang, N., Zhang, Z.M., Liu, L., Zhang, C., Zhang, Y.L. and Zhang, Z.C. Effects of Ca^{2+} channel blockers on store-operated Ca^{2+} channel currents of Kupffer cells after hepatic ischemia/reperfusion injury in rats. *World J. Gastroenterol.* 12: 4694-4698, 2006.
21. Kurita, M., Shimauchi, T., Kobayashi, M., Atarashi, K., Mori, K. and Tokura, Y. Induction of keratinocyte apoptosis by photosensitizing chemicals plus UVA. *J. Dermatol. Sci.* 45: 105-112, 2007.
22. Lettéron, P., Degott, C., Labbe, G., Larrey, D., Descatoire, V., Tinel, M. and Pessayre, D. Methoxsalen decreases the metabolic activation and prevents the hepatotoxicity and nephrotoxicity of chloroform in mice. *Toxicol. Appl. Pharmacol.* 91: 266-273, 1987.
23. Letteron, P., Descatoire, V., Larrey, D., DeGott, C., Tinel, M., Geneve, J. and Pessayre, D. Pre- or post-treatment with methoxsalen prevents the hepatotoxicity of acetaminophen in mice. *J. Pharmacol. Exp. Ther.* 239: 559-567, 1986.
24. Lin, K.L., Chi, C.C., Lu, T., Tseng, L.L., Wang, J.L., Lu, Y.C. and Jan,

C.R. Effect of sertraline on $[Ca^{2+}]_i$ and viability of human MG63 osteosarcoma cells. *Drug Chem. Toxicol.* 36: 231-240, 2013.
25. Lu, Y.C., Chen, I.S., Chou, C.T., Huang, J.K., Chang, H.T., Tsai, J.Y., Hsu, S.S., Liao, W.C., Wang, J.L., Lin, K.L., Liu, S.I., Kuo, C.C., Ho, C.M. and Jan, C.R. 3,3'-Diindolylmethane alters Ca^{2+} homeostasis and viability in MG63 human osteosarcoma cells. *Basic Clin. Pharmacol. Toxicol.* 110: 314-321, 2012.
26. Luo, M. and Anderson, M.E. Mechanisms of altered Ca^{2+} handling in heart failure. *Circ. Res.* 113: 690-708, 2013.
27. Martelli, A.M., Cappellini, A., Tazzari, P.L., Billi, A.M., Tassi, C., Ricci, F., Falà, F. and Conte, R. Caspase-9 is the upstream caspase activated by 8-methoxypsoralen and ultraviolet-A radiation treatment of Jurkat T leukemia cells and normal T lymphocytes. *Haematologica* 89: 471-479, 2004.
28. Merritt, J.E., Jacob, R. and Hallam, T.J. Use of manganese to discriminate between calcium influx and mobilization from internal stores in stimulated human neutrophils. *J. Biol. Chem.* 264: 1522-1527, 1989.
29. Ojala, T., Vuorela, P., Vuorela, H. and Törnquist, K. The coumarin osthol attenuates the binding of thyrotropin-releasing hormone in rat pituitary GH4C1 cells. *Planta Med.* 67: 236-239, 2001.
30. Peng, Y., Liu, W., Xiong, J., Gui, H.Y., Feng, X.M., Chen, R.N., Hu, G. and Yang, J. Down regulation of differentiated embryonic chondrocytes 1 (DEC1) is involved in 8-methoxypsoralen-induced apoptosis in HepG2 cells. *Toxicology* 301: 58-65, 2012.
31. Putney, J.W. Jr. A model for receptor-regulated calcium entry. *Cell Calcium* 7: 1-12, 1986.
32. Quinn, T., Molloy, M., Smyth, A. and Baird, A.W. Capacitative calcium entry in guinea pig gallbladder smooth muscle *in vitro*. *Life Sci.* 74: 1659-1669, 2004.
33. Roelandts R. Mutagenicity and carcinogenicity of methoxsalen plus UV-A. *Arch. Dermatol.* 120: 662-669, 1984.
34. Schmitz, F., Natarajan, S., Venkatesan, J.K., Wahl, S., Schwarz, K. and Grabner, C.P. EF hand-mediated Ca- and cGMP-signaling in photoreceptor synaptic terminals. *Front. Mol. Neurosci.* 5: 26, 2012.
35. Shideman, C.R., Reinardy, J.L. and Thayer, S.A. gamma-Secretase activity modulates store-operated Ca^{2+} entry into rat sensory neurons. *Neurosci. Lett.* 451: 124-128, 2009.
36. Smedler, E. and Uhlén, P. Frequency decoding of calcium oscillations. *Biochim. Biophys. Acta* 1840: 964-969, 2014.
37. Stadler, K., Frey, B., Munoz, L.E., Finzel, S., Rech, J., Fietkau, R., Herrmann, M., Hueber, A. and Gaipl, U.S. Photopheresis with UV-A light and 8-methoxypsoralen leads to cell death and to release of blebs with anti-inflammatory phenotype in activated and non-activated lymphocytes. *Biochem. Biophys. Res. Commun.* 386: 71-76, 2009.
38. Thompson, A.K., Mostafapour, S.P., Denlinger, L.C., Bleasdale, J.E. and Fisher, S.K. The aminosteroid U-73122 inhibits muscarinic receptor sequestration and phosphoinositide hydrolysis in SK-N-SH neuroblastoma cells. A role for Gp in receptor compartmentation. *J. Biol. Chem.* 266: 23856-23862, 1991.
39. Tian, W., Cai, J., Xu, Y., Luo, X., Zhang, J., Zhang, Z., Zhang, Q., Wang, X., Hu, L. and Lin, G. Determination of xanthotoxin using a liquid chromatography-mass spectrometry and its application to pharmacokinetics and tissue distribution model in rat. *Int. J. Clin. Exp. Med.* 8: 15164-15172, 2015.
40. Tsien, R.Y. New calcium indicators and buffers with high selectivity against magnesium and protons: design, synthesis, and properties of prototype structures. *Biochemistry* 19: 2396-2404, 1980.
41. Van Esch, G.J. Toxicology of tert-butylhydroquinone (TBHQ). *Food Chem. Toxicol.* 24: 1063-1065, 1986.
42. Viola, G., Fortunato, E., Cecconet, L., Del Giudice, L., Dall'Acqua, F. and Basso, G. Central role of mitochondria and p53 in PUVA-induced apoptosis in human keratinocytes cell line NCTC-2544. *Toxicol. Appl. Pharmacol.* 227: 84-96, 2008.
43. von Weymarn, L.B., Zhang, Q.Y., Ding, X. and Hollenberg, P.F. Effects of 8-methoxypsoralen on cytochrome P450 2A13. *Carcinogenesis* 26: 621-629, 2005.
44. Wolnicka-Glubisz, A., Fraczek, J., Skrzeczynska-Moncznik, J., Friedlein, G., Mikolajczyk, T., Sarna, T. and Pryjma, J. Effect of UVA and 8-methoxypsoralen, 4, 6, 4'-trimethylangelicin or chlorpromazine on apoptosis of lymphocytes and their recognition by monocytes. *J. Physiol. Pharmacol.* 61: 107-114, 2010.
45. Zhao, G., Peng, C., Du, W. and Wang, S. Pharmacokinetic study of eight coumarins of Radix Angelicae Dahuricae in rats by gas chromatography-mass spectrometry. *Fitoterapia* 89: 250-256, 2013.